# Electronic Supplementary Information

## Surfactant-mediated enhanced FRET from a quantum-dot complex for ratiometric sensing of food colorants

Sumit Singha,[a, ǂ] Mihir Manna,[b, ǂ] Priya Das,[c] Sabyasachi Pramanik,[d,*] & Satyapriya Bhandari [a,*]

[a]Department of Chemistry, University of North Bengal, Darjeeling, West Bengal – 734013, India.
[b]Centre for Nanotechnology, Indian Institute of Technology Guwahati, Assam-781039, India.
[c]Department of Chemistry, Indian Institute of Technology Guwahati, Assam-781039, India.
[d]Assam Energy Institute (Centre of Rajiv Gandhi Institute of Petroleum Technology), Sivasagar, Assam–785697, India.

[ǂ] Authors contributed equally.

*** Corresponding Author E-mails:** satyapriya@nbu.ac.in; spramanik@rgipt.ac.in

### Experimental Section:

**A. Materials**: Zinc acetate dihydrate (99%, Merck), sodium sulphide (58%, Merck), 8-hydroxyquinoline (HQ; Merck), cetyltrimethylammoniumbromide (CTAB), rhodamine B (RhB; ≥ 98%, Sigma), quinine sulfate (Fluka), sulphuric acid (Merck), sodium hydroxide (Merck), sucrose (Merck), glucose (Merck), glutamin (Merck), glycine (Merck), citric acid (Merck), ascorbic acid (Merck), and salts of $Mg^{2+}$, $Ca^{2+}$, $Zn^{2+}$, $Na^{+}$, and $K^{+}$ (Merck), are procured and used as they received. Mili-Q grade water is used in all experiments.

**B. Synthesis of QDs, QDCs, and S-QDCs: (i) Synthesis of ZnS QDs:** ZnS QDs are synthesized using an earlier reported protocol.[S1-S4] In short, to an aqueous mixture of 5.0 mM zinc acetate dihydrate, a 5.0 mM sodium sulfide is added in 50.0 mL of Mili-Q water and the resulting mixture is heated at 100 °C for 15 min with continuous stirring. The obtained milky white solution is centrifuged two times to discard the unreacted reactants and the separated colloidal particles (i.e., pellet followed by twice centrifugation) pellet is redispersed in 50.0 mL of water for further experiments, morphological and spectroscopic characterizations. **(ii) Synthesis of QDCs:** To a 3.0 mL water dispersion of as-synthesized QDs (having absorbance 0.23 at 330 nm), 30.0 µL of 5.0 mM methanolic solution of 8-hydroxyquinoline (HQ) is added to prepare the QDCs reaction mixture under constant stirring at room temperature.[S2-S4] Then, the obtained reaction mixture is centrifuged to remove the excess HQ and redispersed into the same volume of water for further experiments and morphological and spectroscopic characterizations. **(iii) Synthesis of S-QDCs:** The S-QDCs are prepared by adding 50.0 µL of 50.0 mM of CTAB into 3.0 mL of as-synthesized aqueous solution of QDCs (with absorbance of 0.11 at 365 nm). The resulting mixture is then used for further experiments and morphological and spectroscopic characterizations. For the preparation of S-QDCs, the optimum concentration of CTAB used is calculated to be 0.82 mM. The above-mentioned centrifugation experiments are performed with a speed of 20,000 rpm for 10 minutes.

**C. Preparation of RhB solution:** RhB of strength 0.1, 0.5, and 2.5 mM are prepared by diluting 5 mM stock solution of RhB in methanol and used for further experiment.

**D. FRET Experiments:** RhB is added to an aqueous dispersion of 3.0 mL solution of S-QDCs (having absorbance of 0.11 at 365 nm) so that the final concentrations of RhB are 0.17, 0.33,

0.50, 0.66, 0.99, 1.31, 1.63, 2.45, 3.26, 4.07, 4.89, 6.5, 8.1, 9.7, 13.7, 17.7, 25.6 and 33.5 μM. The emission of the resulting mixture is monitored at an excitation wavelength of 365 nm and each measurement is given a time of 5 minutes. The highest amount of RhB used here is 33.5 μM. The quenching in the emission intensity at 515 nm of S-QDCs, following the addition of RhB in the range of 0.17-33.5 μM, is used to calculate the Stern-Volmer (SV) constant and FRET parameters like (i) overlap integral, (ii) FRET distance, (iii) energy transfer efficiency and donor-acceptor distance. Similar experiments are performed for QDCs in the presence of RhB in the range of 0.17-33.5 μM and consequently the SV constant and mentioned FRET parameters are estimated.

**E. Stern-Volmer (SV) Plot Calculations:** The details of the SV plot's calculation are described as follows: [S4-S6]

$$\frac{Io}{I} = 1 + K_{SV}\,[RhB] \qquad \textbf{(1)}$$

As per equation (1), the values of $K_{SV}$ are as follows:

(a) $K_{SV} = (3.99 \pm 0.045) \times 10^5\ M^{-1}$ for S-QDCs
(b) $K_{SV} = (2.902 \pm 0.035) \times 10^5\ M^{-1}$ for QDCs

**F. FRET Calculations:** The details of the calculation of (i) overlap integral, (ii) FRET distance, (iii) energy transfer efficiency, and donor-acceptor distance are described as follows.[S4-S5] Briefly, the Förster distance $R_o$ (that is the distance upon which 50% FRET is noticed) is calculated using the following equation: [S4-S6]

$$R_o^{\,6} = 8.8 \times 10^{-5} \kappa^2\, \eta^{-4} \emptyset\, J(\lambda)\ (Å^6) \qquad \textbf{(2)}$$

where $\kappa^2$ = orientation factor between the emission dipole of the donor and the absorption dipole of RhB ($\kappa$=2/3; either S-QDCs or QDCs for the current case); $\eta$ = refractive index of the medium ($\eta$ =1.33 for water); $\emptyset$ = photoluminescence quantum yield of the donor [either S-QDCs or QDCs] in absence of RhB, and J ($\lambda$) = overlap integral of the emission spectrum of the donor (either S-QDCs or QDCs) and the absorption spectrum of acceptor RhB.

**(i) Overlap integral:** J ($\lambda$) is calculated using the given formula:

$$J(\lambda) = \frac{\int FD(\lambda)\epsilon(\lambda)\lambda^4 d\lambda}{\int FD(\lambda) d\lambda} \qquad \textbf{(3)}$$

Where, FD ($\lambda$) = corrected emission intensity of donor (either S-QDCs or QDCs) with total intensity normalized to unity, $\varepsilon$ ($\lambda$) = extinction coefficient of RhB. As per equation (3), the values of J ($\lambda$) are as follows:

(a) $J(\lambda) = (2.0348 \pm 0.0023) \times 10^{15}\ M^{-1}\,cm^{-1}nm^4 = (2.0348 \pm 0.0023) \times 10^{-13}\ M^{-1}cm^3$ for S-QDCs
(b) $J(\lambda) = (1.9276 \pm 0.0085) \times 10^{15}\ M^{-1}\,cm^{-1}nm^4 = (1.9276 \pm 0.0085) \times 10^{-13}\ M^{-1}cm^3$ for QDCs

The standard deviation value is obtained followed by performing the experiment in triplicate.

**(ii) FRET-distance:** The Förster distance ($R_0$) is calculated using equations **(2)**

(a) $R_0^6 = (8.8 \times 10^{-5} \times 2/3 \times (1.33)^{-4} \times 0.033 \times 2.03278 \times 10^{15})\ (Å)^6$; $R_0^6 = 1.2556 \times 10^9\ (Å)^6$;

$R_0$ = 32.845 Å = 3.2851 ± 0.0006 nm for S-QDCs
(b) $R_0^6 = (8.8 \times 10^{-5} \times 2/3 \times (1.33)^{-4} \times 0.030 \times 1.98335 \times 10^{15})$ $(Å)^6$; $R_0^6 = 1.1137 \times 10^9$ $(Å)^6$;
$R_0$ = 32.195 Å = 3.2043 ± 0.0023 nm for QDCs

**(iii) Energy transfer efficiency (E):** The energy transfer efficiency is calculated using the following equation:

$$E = 1 - \frac{F_{DA}}{F_D} \qquad \textbf{(4)}$$

Where, $F_{DA}$ = emission intensity of donor (either S-QDCs or QDCs) in the presence of RhB and $F_D$ = emission intensity of donor (either S-QDCs or QDCs) in the absence of RhB. The FRET efficiencies are estimated as follows:

(a) E = 1 - 0.0869 = 0.9131 ± 0.0251 for S-QDCs
(b) E = 1 - 0.2867 = 0.7133 ± 0.0211 for QDCs

**(iv) Donor-acceptor distance:** The donor-acceptor distance ($r_o$) is calculated using the following equation:

$$E = \frac{1}{1+(r_o/R_o)^6} \qquad \textbf{(5)}$$

Where, $r_o$ = distance between donor (either S-QDCs or QDCs) and acceptor RhB and $R_o$ is the Förster distance (the distance at which 50% FRET efficiency is observed). The donor-acceptor distance ($r_o$) at the highest FRET efficiency is estimated as follows:

(a) $r_o$ = 2.2112 ± 0.1204 nm for S-QDCs
(b) $r_o$ = 2.7523 ± 0.0489 nm for QDCs

**G. Calculation of the number of binding constant ($k_b$) and binding sites (n):** The calculation of the number of binding sites and binding constants are based on the following equation: [S4-S6]

$$\log\left(\frac{Io-I}{I}\right) = \log k_b + n \log[RhB] \qquad \textbf{(6)}$$

where $k_b$ is the binding constant and n is the number of binding sites. The linear plots of log $((I_0-I) / I)$ as a function of log [RhB] are shown in Fig. 1D (Manuscript) for S-QDCs and Fig. S7C, (ESI) for QDCs. The estimated binding constants ($k_b$) and binding sites (n) are as follows:

(a) $k_b$ = 6.84 x $10^5$ $M^{-1}$; n = 1.04 ± 0.02 for S-QDCs
(b) $k_b$ = 2.38 x $10^5$ $M^{-1}$; n = 0.985 ± 0.034 for QDCs

**H. Ratiometric visual sensing of RhB:** RhB is added to an aqueous dispersion of 3.0 mL solution of S-QDCs (having absorbance of 0.11 at 365 nm) so that the final concentrations of RhB are 0.17, 0.33, 0.50, 0.66, 0.99, 1.31, 1.63, 2.45, 3.26, 4.07 and 4.89 μM. The emission of the resulting mixture is monitored at an excitation wavelength of 365 nm and each measurement is given a time of 5 minutes. The quenching in the emission intensity of the donor (i.e. S-QDCs) at 515 nm and consequently enhancement in the emission intensity at 576 nm of the acceptor (i.e. RhB) at an excitation wavelength of 365 nm are monitored to describe the ratiometric sensing of RhB. The change in the emission intensity ratio of ($I_{576}/I_{515}$) of S-QDCs in the presence of different concentrations of RhB is used to describe the ratiometric sensing of RhB. This also led to the luminescence color change of S-QDCs from green to yellowish-orange in the presence of

RhB – which clearly describes the visual luminescence change of S-QDCs in the presence of RhB. Each measurement is given a time of 5 minutes. The amount of RhB used here is in the range of 0.16-1.64 μM. The limit of detection (LOD) was estimated by using the $3\sigma/K_{slope}$ equation – which is obtained from the plot of the emission intensity ratio of ($I_{576}/I_{515}$) of S-QDCs vs. concentration of RhB. The experiment is carried out in triplicate. It is to be noted here that $\sigma$ represents the standard deviation of the emission intensity ratio of ($I_{576}/I_{515}$) of S-QDCs and $K_{slope}$ signifies the slope obtained from the plot of the emission intensity ratio of ($I_{576}/I_{515}$) of S-QDCs against the concentration of RhB.

**I. Selectivity experiment:** The selectivity experiment is tested by using 34 times higher concentration (in μM scale) of interfering substances such as (i) $Na^+$, (ii) $K^+$, (iii) $Ca^{2+}$, (iv)$Mg^{2+}$, (v)$Zn^{2+}$, (vi) glucose,(vii) sucrose, (viii) glycine, (ix) citric acid, (x) ascorbic acid, (xi) glutamic acid, (xii) glutamin, and (xiii) RhB in presence of mixture of mentioned substances. The mentioned interfering substances are added to a 3.0 mL solution of S-QDCs (having absorbance of 0.11 at 365 nm) and the emission spectra (at the same excitation wavelength) are recorded. The change in the emission intensity ratio of ($I_{576}/I_{515}$) of S-QDCs is monitored to describe interfering substances of the luminescence of S-QDCs compared to the effect when RhB is added to S-QDCs under the same experimental conditions. This experiment helps to demonstrate the selectivity of S-QDCs towards RhB in the presence of the mentioned interfering substances.

**J. Real Sample Analysis:** Commercial chili powder (Company: Everest and Every Day), tomato ketchup (Company: Kissan), and mixed fruit jam (Company: Kissan) are purchased from the local market and mixed with Mili-Q water under sonication followed by filtration with 0.22 mm syringe filter to obtain the extracts. Briefly, 50.0 mg of chili powders, tomato ketchup, and mixed fruit jam are separately added to 10.0 mL of water and the filtration is performed. The filtrates are used for further experiments. The filtrates are diluted 100 times to prepare the dispersion of S-QDCs in those extracts and are then used for further experiments. Food colorants in those solutions are determined by spiking 0.925 μM of RhB solution to 3.0 mL of S-QDCs (with absorbance of 0.11 at 365 nm) separately and then monitoring the photoluminescence properties of S-QDCs. Notably, a linear relationship between $I_{576}/I_{515}$ of S-QDCs and concentrations of RhB (Fig. 2, Manuscript) is used for the quantification of RhB in commercial chili powders, tomato ketchup, and mixed fruit jam. The results of which are tabulated in Table S3, ESI.

**K. Instruments:** HORIBA Jobin Yvon FluoroMax-4 spectrofluorimeter is mainly used to record photoluminescence and to measure photoluminescence quantum yield (PLQY). Photographs are taken digitally under a spectrofluorimeter. Chromaticity coordinates are calculated by using OSRAM color calculator (CIE-1931) software. PerkinElmer Lambda 35 UV–vis spectrophotometer is used to measure the absorption spectra. The size, shape, and lattice parameters of the QDs, QDCs, and S-QDCs are measured by transmission electron microscopy (TEM; Model: JEOL JEM 2100F, maximum accelerating voltage: 200 kV). Gatan Digital Micrograph software is used for getting inverse fast Fourier transformation images and lattice fringe calculation. Rigaku TTRAX-III X-ray diffractometer is used to measure the X-ray diffraction (XRD) patterns. The pH of the solutions is measured by using a HANNA pH meter. The zeta potential of the samples is measured by Malvern Zetasizer Nano ZS. Time-resolved photoluminescence decay curves are obtained using HORIBA Jobin Yvon spectrofluorimeter (using 375 nm LASER), Model: Ultrafast-01-DD.

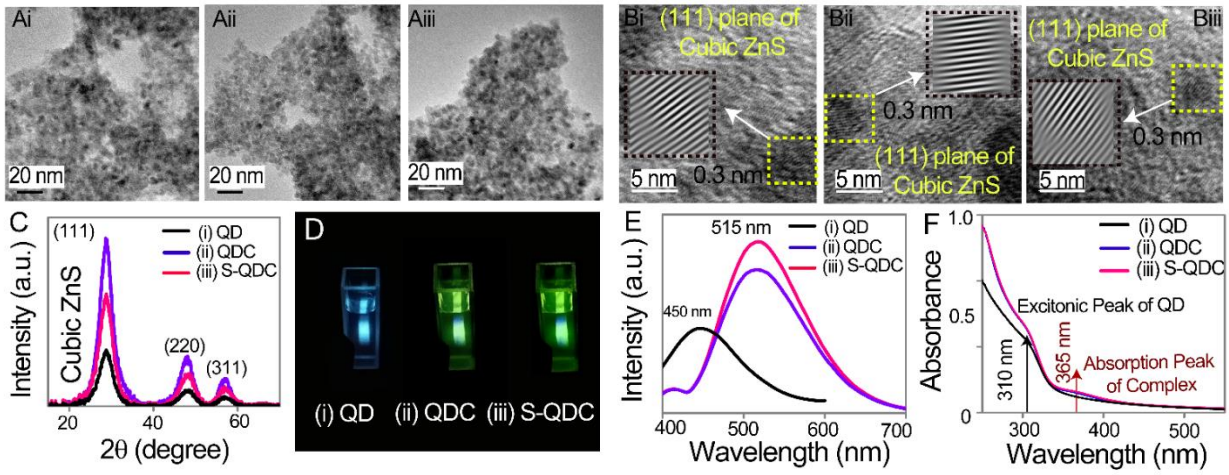


**Fig. S1. (A)** Transmission electron microscopic (TEM) images (scale bar = 20 nm), **(B)** high-resolution TEM images (scale bar = 5 nm) and corresponding inverse fast Fourier transformed (IFFT) analysis (inset), **(C)** thin-film x-ray diffraction patterns, **(D)** digital photographs, **(E)** emission spectra, and **(F)** UV-vis spectra of (i) QDs, (ii) QDCs, and (iii) S-QDCs.

The average particle size of the as-synthesized QDs is 4.0 ± 0.3 nm (Fig. S1Ai). The presence of a 0.3 nm lattice fringe (due to 111 plane of cubic ZnS)[S1-S3] in the high-resolution TEM image and characteristics peaks of (111), (220), and (311) lattice planes of cubic ZnS [S1-S3] in the XRD patterns clearly support the formation of ZnS QDs (Fig. S1B(i) and C(i)). The synthesized ZnS QDs exhibit broad blue emission centered at 450 nm ($\lambda_{ex}$-320 nm; due to the surface trap states) [S1-S3] and an absorption edge at 310 nm (Fig. S1D(i)–F(i)). The results clearly demonstrate the formation of water-soluble ZnS QDs. The QDCs are synthesized followed by reacting QDs with 8-hydroxyquinoline (HQ) ligand leading to the formation of Zn-quinolate complexes on the surface of the QDs, as evidenced by our earlier observations.[S1-S3] The average particle size (4.0 ± 0.3 nm), lattice fringe (0.3 nm) of the major plane (111), and the XRD patterns of cubic ZnS remain preserved after the formation of QDCs (Fig. S1A(ii)–C(ii)). The QDCs display green emission centered at 515 nm ($\lambda_{ex}$-365 nm) and a supplementary absorption peak at 365 nm (due to the formation of Zn-quinolate complex)[S1-S3] in addition to a pristine 310 nm absorption edge ( Fig. S1D(ii)–F(ii)). This clearly indicates the successful formation of QDCs. Then, when the surface of the QDCs is modified with surfactants like CTAB, the formation of S-QDCs, with enhanced luminescence takes place. The morphology in terms of the size, shape, lattice fringe, and XRD patterns of the QDCs remain unaltered when converted to S-QDCs (Fig. S1A(iii)–C(iii)). The S-QDCs exhibit enhanced emission intensity at 515 nm ($\lambda_{ex}$-365 nm) compared to QDCs while the absorption behaviour of the S-QDCs is similar to that of QDCs (Fig. S1E(iii) and F(iii)). The enhancement in emission intensity may be due to the surfactant-induced gaining of the structural rigidity of the Zn-quinolate complex present on the surface of the QDCs, as supported by earlier reports.[S1-S3] The surfactants are attached to the surface of QDCs due to their mutual electrostatic interaction – which is probed by estimating the change in the zeta potential value from 28.27 ± 0.68 mV to 29.73 ± 0.75 mV of QDCs followed by reacting with CTAB to

form S-QDCs (Fig. S2). The used concentration of CTAB is 0.82 mM to construct S-QDCs. The presented results clearly indicate the successful formation of water-soluble highly luminescent S-QDCs. The S-QDCs have a photoluminescence quantum yield (PLQY) of 0.033 at $\lambda_{ex}$-365 nm with regard to quinine-sulphate as a standard (Table S1). Also, the aqueous dispersion of S-QDCs is found to be stable with respect to their luminescence for 48 hours (Fig. S3). This demonstrates the stability of the water-soluble S-QDCs and thus their application potential in sensing purposes.

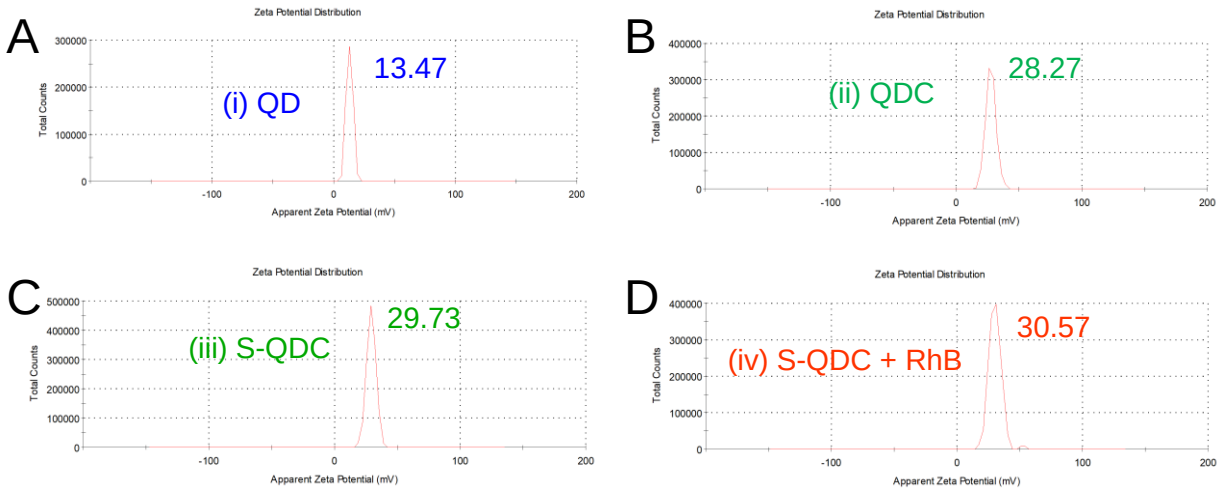


**Fig. S2.** Zeta potential curves of (A) QDs (13.47 ± 0.39 mV), (B) QDCs (28.27 ± 0.68 mV), (C) S-QDCs (29.73 ± 0.75 mV), and (D) RhB treated S-QDCs (30.57 ± 0.25 mV). Notably, the stepwise decrease in the $\Delta\xi$ from QDs to QDCs ($\Delta\zeta$ = 14.8), QDC to S-QDCs ($\Delta\zeta$ = 1.46), and S-QDCs to FRET pair with RhB ($\Delta\zeta$ = 0.84) clearly shows the stepwise increment of positive charges and steric hindrance on the surface of the QDs.

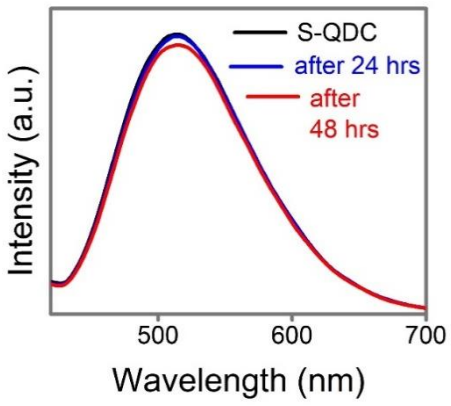


**Fig. S3.** Luminescence stability of S-QDCs in water up to 48 hours.

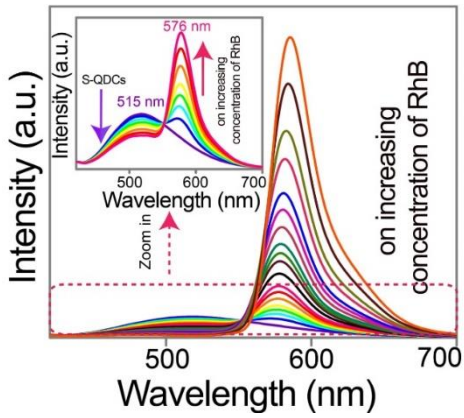


**Fig. S4.** Emission spectra ($\lambda_{ex}$-365 nm) of S-QDCs followed by sequential addition of different concentrations (0-33.55 µM) of RhB. (inset: zoomed version of emission spectra ($\lambda_{ex}$-365 nm) of S-QDCs followed by sequential addition of different concentrations (0.0-1.63 µM) of RhB)

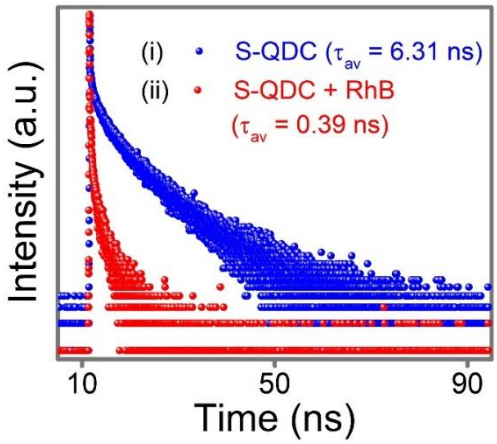


**Fig. S5.** Photoluminescence decay profile ($\lambda_{ex}$= 375 nm) of S-QDCs at 515 nm (i) before and (ii) after 33.55 µM RhB treatment. The reduction in the average lifetime value of the S-QDCs (at 515 nm) in the presence of RhB indicates strong dynamic quenching and also helps to estimate the energy transfer efficiency – which is well matched with the energy transfer efficiency as calculated using the changes in the emission intensity of the S-QDCs and subsequently ruled out the possibility of inner filter effects of RhB in the FRET Pair (Fig. S5 and Table S2, ESI).

**Energy transfer efficiency (E) from average lifetime values:** The energy transfer efficiency is calculated using the following equation:

$$E = 1 - \frac{T_{DA}}{T_D} \qquad \textbf{(7)}$$

Where, $T_{DA}$ = average lifetime of the donor (here S-QDCs) in the presence of acceptor (here RhB) and $T_D$ = average lifetime of the donor (here S-QDCs) in the absence of acceptor (here RhB). The FRET efficiency is estimated as follows:

E = 1 - 0.0618 = 0.9382 for S-QDCs

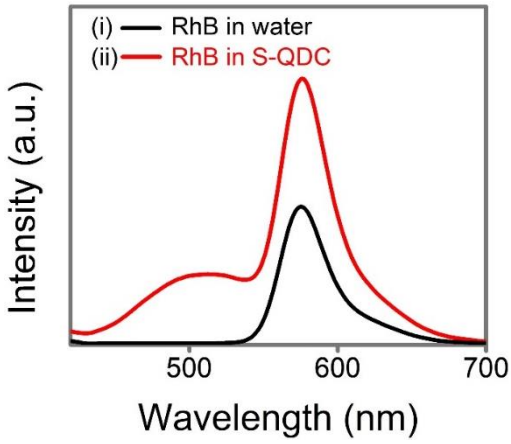


**Fig. S6.** Comparison of the emission spectra ($\lambda_{ex}$= 365 nm) of 1.63 µM RhB in (i) water and (ii) S-QDCs dispersion.

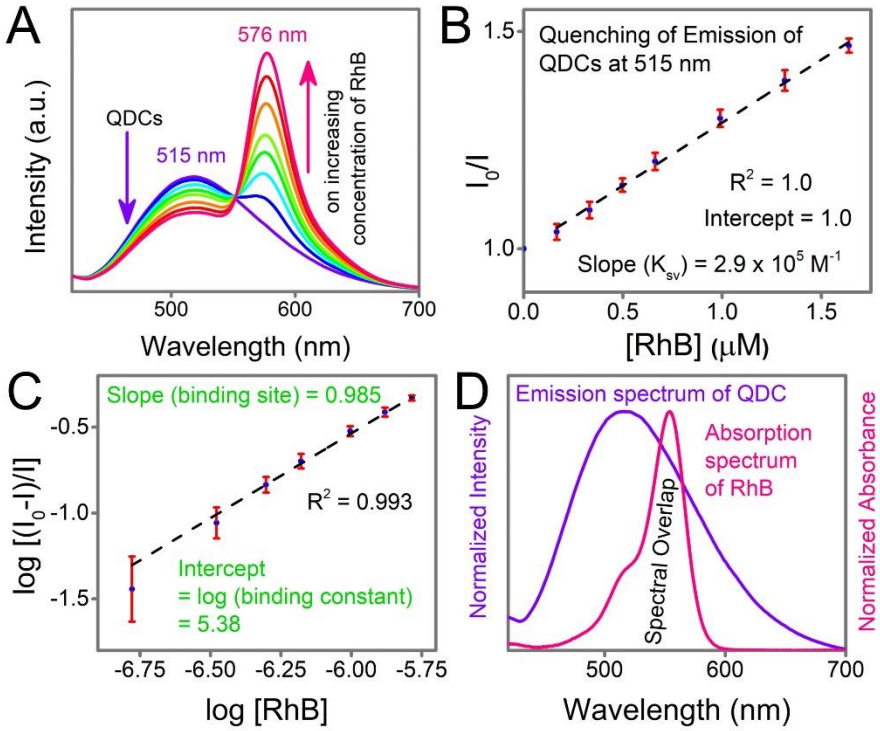


**Fig. S7. (A)** Emission spectra ($\lambda_{ex}$-365 nm) of QDCs followed by sequential addition of different concentrations (0-1.64 µM) of RhB. **(B)** Linear Stern-Volmer plot and **(C)** plot of log (($I_0$-I)/I) vs log [RhB] for QDCs with different concentrations of RhB (using Fig. S7 (A)). **(D)** Spectral overlap of the emission spectrum of QDCs ($\lambda_{ex}$-365 nm) with the absorption spectrum of RhB.

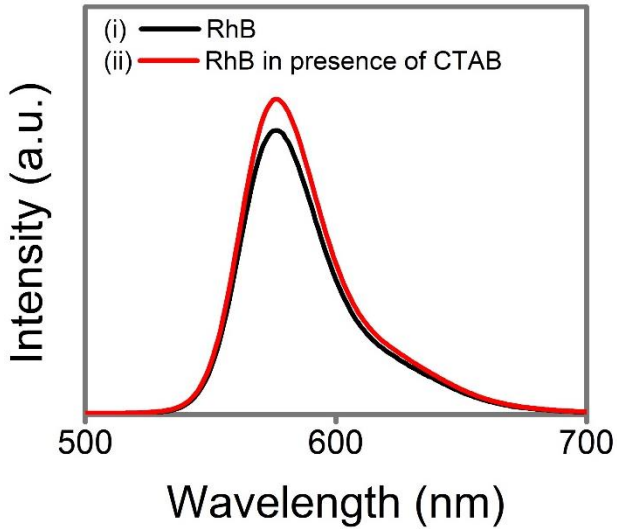


**Fig. S8. E**mission spectra ($\lambda_{ex}$= 365 nm) of RhB in (i) absence and (ii) presence of CTAB. Also, a small enhancement in the emission intensity at 576 nm is noticed when CTAB is added to only RhB, thus further supporting the auxiliary role of CTAB towards the attachment of RhB on the sterically hindered surface of the S-QDCs.

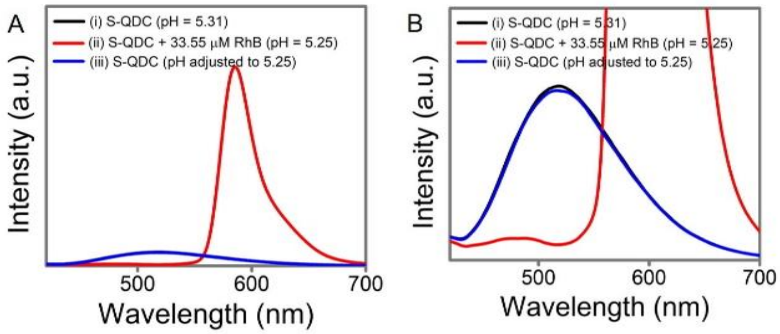


**Fig. S9. (A)** Emission spectra ($\lambda_{ex}$= 365 nm) of S-QDCs (i) before (pH-5.31) and (ii) after RhB (33.55 µM) treatment (pH-5.25) and (iii) S-QDCs adjusted to pH = 5.25 (i.e., the same pH of S-QDCs followed by treatment of RhB). **(B)** Y-axis magnified emission spectra against Fig. S9A to see the effect of pH on the emission of S-QDCs at 515 nm. When the pH of the S-QDCs (pH = 5.31) was adjusted to the pH of the RhB-added S-QDCs (pH = 5.25), there was no significant change in the emission spectrum of the S-QDCs. This evidently ruled out the probability of the pH effect on the observed changes in the emission of the S-QDCs upon RhB treatment.

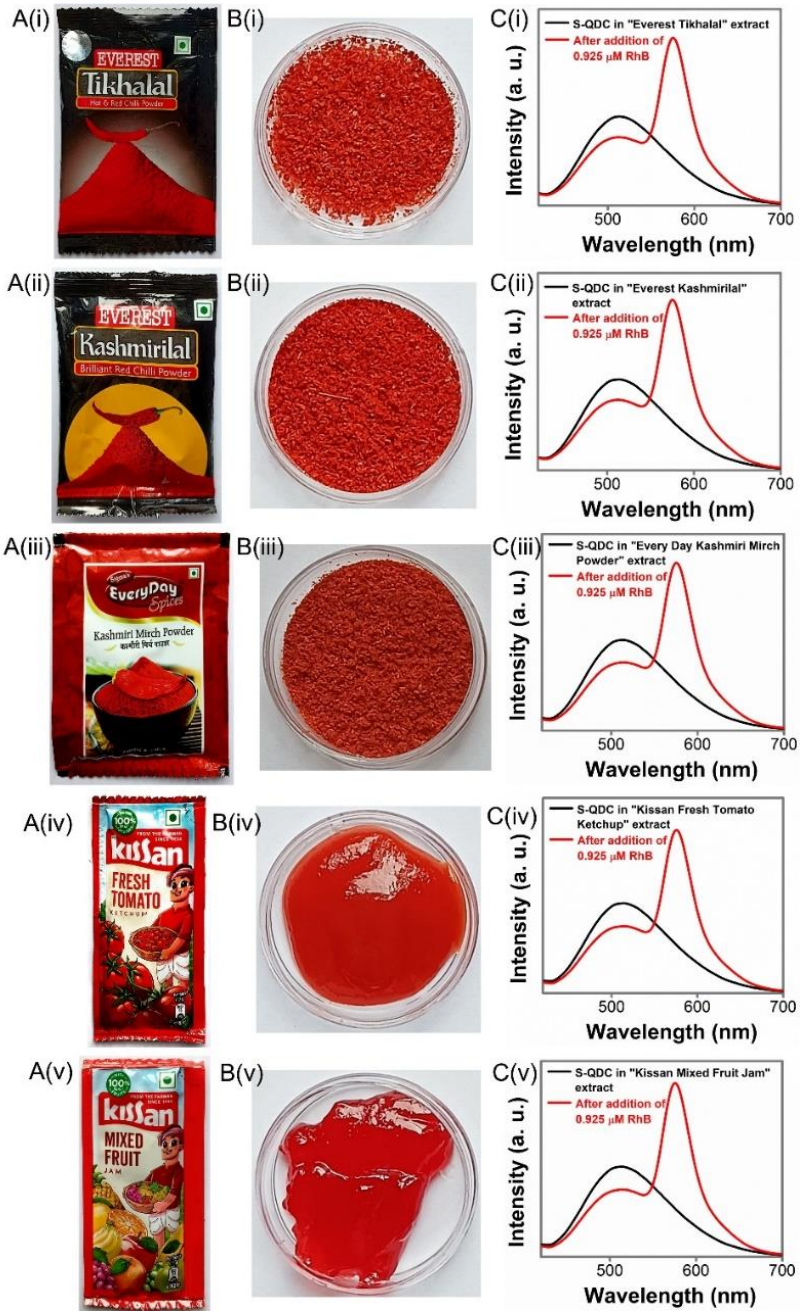


**Fig. S10. (A)** Digital photographs of the packet of commercialized foodstuffs as purchased from the market, **(B)** digital photographs of the foodstuffs inside the packet taken out and placed in a Petri plate, **(C)** representative emission spectra ($\lambda_{ex}$= 365 nm) of S-QDCs in the extract of the (i) chili powder "Tikhalal" (Company: Everest), (ii) chili powder "Kashmirilal" (Company: Everest), (iii) chili powder "Kashmiri Mirch Powder" (Company: Every Day), (iv) tomato ketchup (Company: Kissan) and (v) mixed fruit jam (Company: Kissan) following the spiking of 0.925 μM of RhB.

**Table S1.** Tabulated form of photoluminescence quantum yields of QDCs and S-QDCs at an excitation wavelength of 365 nm with respect to quinine sulphate.

| Samples | | PLQY |
|---|---|---|
| (i) | QDCs | 0.030 |
| (ii) | S-QDCs | 0.033 |

**Table S2.** Tabulated form of the average lifetimes obtained from the time-resolved photoluminescence spectra ($\lambda_{ex}$ = 375 nm) of S-QDCs monitored at 515 nm in (i) absence and (ii) presence of the highest amount of RhB.

| Samples | $\alpha_1$ (%) | $\tau_1$ (ns) | $\alpha_2$ (%) | $\tau_2$ (ns) | $\alpha_3$ (%) | $\tau_3$ (ns) | $\tau_{av}$ (ns) | $\chi^2$ |
|---|---|---|---|---|---|---|---|---|
| S-QDCs | 2.80 | 2.05 | 1.43 | 9.57 | 95.77 | 0.0336 | 6.31 | 1.08 |
| S-QDCs+ RhB | 0.32 | 0.43 | 0.10 | 2.50 | 99.58 | 0.0141 | 0.39 | 1.05 |

**Table S3.** Tabulated form of the comparison of optical sensors/other methods for sensing RhB which presents as a food colorant.

| Ref. No. | Used optical nanoprobe/methods | Linear range | LOD |
|---|---|---|---|
| This work | S-QDCs | 0.17-4.89 μM<br>81.4-2342.4 μg $L^{-1}$ | 2.2 nM<br>1.05 μg $L^{-1}$ |
| Ref. S7 | b-CD-AuNPs/HCNS nanohybrids | 4.79–958.00 μg $L^{-1}$ | 0.96 μg $L^{-1}$ |
| Ref. S8 | 3D-RGO composite | 0.025 to 150 μg $L^{-1}$ | 0.0074 μg $L^{-1}$ |
| Ref. S9 | $Fe_3O_4$/ANI-NA | 0.35–5.00 μg $L^{-1}$ | 0.10 μg $L^{-1}$ |
| Ref. S10 | Cloud point extraction (CPE) | 0.0467 - 100 μg $L^{-1}$ | 0.014 μg $L^{-1}$ |
| Ref. S11 | $Fe_3O_4$@MIPs/ MIPs–SPE–HPLC | 100–8000 μg $L^{-1}$ | 3.4 μg $L^{-1}$ |
| Ref. S12 | Sepabeads SP 70 resin/ SPE–UV | 250–3000 μg $L^{-1}$ | 3.14 μg $L^{-1}$ |
| Ref. S13 | Ionic liquid/ DLLME–FO–LADS | 5–100 μg $L^{-1}$ | 1.05 μg $L^{-1}$ |

**Table S4.** Results for detection of food colorants in commercial chili powder, tomato ketchup, and mixed fruit jam.

| Sample S-QDCs in extract of | Spiked (μM) | Calculated (μM) | Recovery (%) ± RSD |
|---|---|---|---|
| (i) Tikhalal chili powder | 0.925 | 0.904 | 97.73 ± 1.19 |
| (ii) Kashmirilal chili powder | 0.925 | 0.889 | 96.11 ± 1.30 |
| (iii) Kashmiri chili powder | 0.925 | 0.897 | 96.97 ± 0.65 |
| (iv) Tomato ketchup | 0.925 | 0.889 | 96.11 ± 0.76 |
| (v) Mixed fruit jam | 0.925 | 0.956 | 103.35 ± 0.76 |

**References:**


**S1).** S. Pramanik, S. Roy, A. Mondal and S. Bhandari, *Chem. Commun*., 2019, **55**, 4331-4334.

**S2).** M. Manna, S. Roy, S. Bhandari and A. Chattopadhyay, *J. Mater. Chem. C*, 2021, **9**, 13810-13817.

**S3).** M. Manna, S. Roy, S. Bhandari and A. Chattopadhyay, *J. Mater. Chem. C*, 2020, **8**, 6972-6976.

**S4).** S. Pramanik, S. Roy, A. Mondal and S. Bhandari, *Nanoscale Adv.*, 2020, **2**, 3809-3814.

**S5).** V.V. Koppal, P.G. Patil, R. M. Melavanki, R. A. Kusanur, U. O. Afi and N.R. Patil, *J. Mol. Liq.*, 2019, **292**, 111419.

**S6).** A. Jaiswal, P. Sanpui, A. Chattopadhyay and S. S. Ghosh, *Plasmonics* 2011, **6**, 125.

**S7).** Y. Yi, H. Sun, G. Zhu, Z. Zhang and X. Wu, *Anal. Methods*, 2015, **7**, 4965-4970.

**S8).** J. Yan, J. M. Cen, X. C. Tan, S. F. Tan, Y. Y. Wu, H. Zhang and Q. Wang, *Anal. Methods*, 2017, **9**, 5433-5440.

**S9).** H. Bagheri, R. Daliri and A. Roostaie, *Anal. Chim. Acta*, 2013, **794**, 38–46.

**S10).** M. Alesso, G. Bondioli, M. C. Talio, M. O. Luconi and L. P. Fernandez, *Food Chem*., 2012, **134**, 513-517.

**S11).** X. Su, X. Li, M. Liu, F. Lei, X. Tan, P. Li and W. Luo, *Food Chem*., 2015, **171**, 292–297.

**S12).** M. Soylak, Y. E. Unsal, E. Yilmaz and M. Tuzen, *Food Chem. Toxicol*., 2011, **49**, 1796–1799.

**S13).** M. Taziki, F. Shemirani and B. Majidi, *Sep. Purif. Technol.*, 2012, **97**, 216–220.